Numerical Analysis of an Isolated Main Helicopter Rotor in Hovering and Forward Flight

Nik Ahmad Ridhwan Nik Mohd[i] and Abas Ab. Wahab[ii]
Dept. of Aeronautic and Automotive Eng.,
Faculty of Mechanical Engineering,Universiti Teknologi Malaysia,
81300 Skudai, Johor,Malaysia.
Tel: +607-5534879, Fax: +607-5566159

Abstract: Aerodynamic characteristics of a 5-seater helicopter with different rotor configuration (i.e.; blade number and size) operating in forward flight mode were simulated by using commercial computational fluid dynamic (CFD) software called FLUENT. The main objective of this simulation is to calculate the aerodynamic load generated by rotor during hovering and different forward flight speed range. The effects of using different rotor configuration and shaft rotational speed (different engine selection) includes in this simulation. For CFD analysis, the multiple references rotating frame method (MRF) with standard viscous k-ε turbulent flow model was used on modelling the rotating rotor operating both in hovering and forward flight. To simulate the helicopter operating in the trim condition, the main rotor collective pitch, coning and flapping angle was calculated based on the blade element theory (BET). The blade is assumed stationary and blade collective pitch, coning and flapping angle was positioned as calculated using BET. For this purpose CFD simulation has been compared with the corresponding results obtained from BET analysis and that found they were in good agreements.
Keywords: aerodynamic, CFD, helicopter, performance, rotor blade

1.0 Introduction

Nowadays CFD analysis is so versatile, it was used to investigate the flow about almost type of vehicle, including rotorcraft. Long before computers were available to perform a large number of lengthy calculations in a short period of time, aeronautical engineers used three primary methods of investigation to visualize the flowfield around a flight vehicle. The earliest methods for modelling rotors were based on an extension of Prandtl's lifting line theory for wings. In these techniques, the individual blades were modelled as line vortices, and the wake was modelled as a deformed helix.

Flight tests are extremely expensive and time consuming while the solutions found are often alter rather than optimised configurations. The wind tunnel methodology can be more efficient for conventional problems such as fuselage drag reduction but many low speed interactional conditions have been found difficult to test with sufficient confidence. The helicopter industry is therefore increasingly using CFD methods by incorporating them in its design environment in order to reduce the number of wind tunnel tests and to increase the number of configurations being explored numerically.

Numerous CFD techniques were introduced for calculating the airloads acting on helicopter blade and simulate flow over the helicopter rotors. During 1970s and 1980's, these methods were augmented by modern CFD techniques. Caradonna and Isom [1] applied the transonic small disturbance theory to lifting rotors and Chang [2] modified the full potential flow solver FLO22 for isolated wings to model rotors. The WIND code developed by NASA Glenn Research Center was used on simulating the turbulent flow past the robin helicopter with four-bladed rotor [3]. In this work, the entire configuration of helicopter was modelled with Chimera multi-block mesh and the individual blade was modelled with Chimera moving grid in quasi-steady flow-field. The k-ω SST turbulence model was used. Using the Navier-Stokes overset grid methodologies employed here, Strawn [4] showed good performance prediction for a 4-bladed UH-60 rotor. Furthermore, in this Franco-German program on simulating the isolated rotor in forward flight, ONERA Euler method uses a deforming grid strategy and DLR is based on Chimera grid method [5]. Another approach that was applied on simulating aerodynamic characteristics of complete helicopter and that was presented in this paper is based on the simulation performed by Fluent on Apache attack helicopter during hovering flight. The main rotor blade was modelled by using sliding mesh method and tail rotor however was simulated by using the Multiple References Rotating Frame (MRF) method [6].

Using the standard k-ε turbulent flow model, the rotor will be simulated using MRF method and the capability of FLUENT software on simulating helicopter rotor blade in hovering and forward flight will be evaluated.

i MSc Student, email: ridhwan@fkm.utm.my
ii Lecturer, Prof, Ir. Dr., email: ridhwan@fkm.utm.my

2.0 Methodology

The aerodynamic load (i.e.; lift and drag) of complete helicopter with different rotor configurations was analysed. By concerning the effect of rotor downwash, the total fuselage drag of the helicopter was calculated based on the equivalent flat plate area and the isolated rotor drag was simulated using MRF method offered by FLUENT. The selection of this simulation method is made based on the previous work that has been done by FLUENT on simulating the complete Apache attack helicopter [1]. Furthermore, the isolated helicopter rotor blade was simulated from hovering mode to the maximum allowable cruising flight speed as calculated using BET.

During forward flight, the helicopter main rotor blades is dynamically flapping, and pitching about the rotational axis. The lack of expertise to modelling this dynamic motion, the blade is assumed stationary while the fluid is assumed rotating in the reference rotational axis. To ensure the flow encountered by every blade is in actual condition, all the main rotor blade at every azimuth angle was set to the correct pitch and coning angle as calculated using BET (Table 1). This technique will seems equivalent to the dynamically flapping rotor blade rotating at its rotational axis. In this simulation the rotational axis is different correspond to the forward flight speed and the rotor tip path plane (TPP).

The helicopter main rotor blade flapping coefficient (i.e.; longitudinal flapping, a_n and lateral flapping, b_n), rotor coning angle, a_o and the cyclic pitch coefficient (i.e.; longitudinal cyclic, B_1 and lateral cyclic, A_1) as a function of blade azimuth angle, Ψ can respectively be modelled using Eq. 1 and Eq. 2 [7,8]. By allowing the blade to freely flapping about its rotational axis, this phenomenon permit both the blade at advancing and retreating side to produce equal amount of lift force to encounter the asymmetry of flow field generated in both rotor blade sides.

$$\beta(\Psi) = a_0 - \sum_{n=1}^{\infty}\left(a_{n_s}\cos n\Psi - b_{n_s}\sin n\Psi\right) \quad \text{(Eq. 1)}$$

$$\theta(r,\Psi) = \theta_o + \frac{r}{R}\theta_{tw} - A_1\cos\Psi - B_1\sin\Psi \quad \text{(Eq. 2)}$$

The sectional blade angle of attack can be measured using Eq. 3;

$$\alpha(\bar{r},\Psi) = \frac{1}{\bar{r}+\mu\sin\Psi}\left\{\begin{array}{l}\bar{r}\left[\theta_o + \theta_1\bar{r} - \overline{A}\cos\Psi - \overline{B}\sin\Psi\right] - \dfrac{v}{\Omega R}\left(1+\bar{r}\cos\Psi\right)\\ +\mu\left[\alpha_{TPP} + \left(\theta_o + \theta_1\bar{r}\right)\sin\Psi - a_o\cos\Psi - \overline{A}\sin\Psi\cos\Psi - \overline{B}\sin^2\Psi\right]\end{array}\right\} \quad \text{(Eq. 3)}$$

where $\overline{A} = A_1 - b_{1_s}$, $\overline{B} = B_1 - a_{1_s}$, $\bar{r} = r/R$, collective pitch, θ_o and angle of tip path plane, α_{TPP}.

In CFD analysis, the computational domain (or control volume) used is based on the closed-test section wind tunnel. The appropriate computational domain and selection of boundary conditios were made based on the simulation performed at Georgia Institute of Technology (GIT) on simulating rotor wake and body interaction [9]. The bigger ratio between computational domain and rotor size was used to minimize the blockage effect or wall boundary effect particularly below the rotating rotor where the airflow induced downstream by rotor. The appropriate height between rotor and the bottom wall boundary is important because it may increase the effect of ground to the rotor performance. For that reason, the helicopter rotor of radius R = 5.345 m and R = 4.80 m was simulated in the computational domain with the clearance size of A = 5R, B = 10R, C = 20R, D = 15R and E = 10R between rotor and upper wall (A), bottom wall (B), pressure outlet boundary (C), Velocity inlet boundary (D) and port and starboard wall boundary (E). The rotor rotational speed, Ω for rotor of 5.345 m and 4.80 m radius was set to 394 rpm and 413.74 rpm respectively. Speed at inlet boundary condition was set to zero for static flight condition to the maximum continuous attainable flight speed for every rotor configurations.

In pre-processing stage, both the blade and the computational domain were meshed using tetrahedral grid type. Table 2 depicts the size of grid used for 3-bladed rotor simulation.

Table 1: Dynamic coefficient and performance table of helicopter with Different Blade-engine Combinations.

Combination	Manual[14]	(A)	(B)	(C)	(D)
Collective pitch required (Deg.)	-	15.64	16.79	18.10	20.62
Angle of tip path plane, TPP (Deg.)	-	-5.91	-9.67	-6.72	-10.50
Longitudinal cyclic pitch (Deg.)	-	9.05	14.44	12.07	17.67
Lateral cyclic pitch (Deg.)	-	0	0	0	0
Longitudinal flapping	-	-3.91	-7.67	-4.72	-8.497
Lateral flapping (Deg.)	-	1.62	1.62	1.71	1.70

Table 2: Grid Size used for 3-bladed Rotor Simulation

```
Grid Size

Level    Cells    Faces    Nodes   Partitions
    0   764623  1583651   164266           1

 2 cell zones, 7 face zones.
```

The solver setting must be done correctly. In this simulation, the large ratio of computational domain to the rotor diameter was applied. The absolute velocity formulation was chosen where where the most of the flow inside the computational domain is irrotational. For residual convergence stabilisation purposes, the under relaxation factors for pressure was reduced by 33% and for momentum, turbulent kinetic energy, and turbulent dissipation were reduced by 44%. Table 3 and 4 represent four possible blade and engine configuration that can be used on improving the forward flight speed of single rotor helicopter. The same configuration was also used in this study.

Table 3: Current and Proposed Configuration of Eurocopter AS 355F2 Blade and Engine.

Eurocopter AS 355F2		
	Blade	**Engine**
Current configuration	**Radius: 5.345m Chord : 0.35m Airfoil : Onera 209 Number of blade: 3**	**Allison C250-20F Power: 450 shp Ω output: 6016 rpm**
New configuration	**Radius: 4.80m Chord : 0.31m Airfoil : Onera 209 Number of blade: 4**	**Allison C250-47B Power: 650 shp Ω output: 6317 rpm**

Table 4: Combination between Blade and Engine.

Design Approach				
	Blade		**Engine**	
Combination	**Current**	**New**	**Current**	**New**
(A)	√		√	
(B)	√			√
(C)		√	√	
(D)		√		√

3.0 Result and Discussion

The analysis of isolated helicopter rotor using CFD method was performed only to the rotor-engine with combination (A) and (B). Combination (A) is the existing configuration of rotor and engine. Simulation was firstly done on combination (A) to the technique and method used is correct. From previous analysis have been done to combination (C) and (D), there is no improvement on helicopter cruising or forward flight speed performance. Because of that reason, all data relating to combination (C) and (D) will not representing here.

Calculating the aerodynamic loads (i.e.; lift and drag) acting on the rotor blade as a whole is not a direct calculation. This is because the forces obtained from CFD analysis are the forces generated by isolated rotor. Further calculation concerning fuselage aerodynamic was carried-out. Combining these two sources of aerodynamic force will provide a data for a complete helicopter. According to the Table 5 and 6, the calculated (BET) lift force, L_M produced by the rotor of a complete helicopter shows a constant value for all range of flight speed. This situation occurs to ensure that the helicopter in this study will perform a steady and level flight. The constant increment in lift force, L_M represent in CFD column is due to the lift generate by the isolated rotor. A high percentage of error was perceived on CFD simulation result when the speed of flight was increased greater than 20m/s. This error is expected to come from many of sources such as meshing technique, number of nodes used and the selection of appropriate turbulent flow model. Other high degree of error also may come from the method of simulation where the rotor dynamic motion was ignored here. In static or hovering flight, the high accuracy of lift and drag force (3.0% to 9.5%) was observed both for BET and CFD.

Table 5: Aerodynamic Loads of Combination (A) obtained from BET and CFD Analysis.

	BET		CFD		Variance (%)	
V_∞	L_M	H_M	L_M	H_M	L_M	H_M
0	**24917.4**	**382.86**	**26753.3**	**408.1**	**5.36**	**6.6**
20	**24917.4**	**1331.6**	**27789.9**	**1404.1**	**9.52**	**5.17**
40	**24917.4**	**2670.6**	**29018.7**	**2877.0**	**13.16**	**7.17**
67.15	**24917.4**	**4481.0**	**30648.0**	**4917.6**	**16.18**	**8.88**

Table 6: Aerodynamic Loads of Combination (B) obtained from BET and CFD Analysis.

	BET		CFD		Variance (%)	
V_∞	L_M	H_M	L_M	H_M	L_M	H_M
0	24999. 2	268.14	26021.1	289.6	3.05	8.0
20	24999. 2	1589.5	27261.4	1703.4	7.53	6.69
40	24999. 2	3138.1	28949.7	3348.1	12.80	6.27
60	24999. 2	4663.3	28906.1	5070.0	11.89	8.02
89.76	24999. 2	7031.6	31162.7	7690.1	15.62	8.56

Illustrated in Fig. 1 and Fig. 2 are the contour of velocity magnitude of 3-bladed rotor at hovering flight mode that respectively captured from plan and side view. From Fig. 1, the expected axisymmetrical velocity distribution was generated by the blade. The axisymmetric on velocity distribution is particularly due to equivalent on the tip speed experienced by every blade at any arbitrary azimuth angle. At forward flight, the inherent asymmetric nature of flow over the rotor disc gives rise to a number of aerodynamic problems that ultimately limit the rotor performance. As the flight speed is increased (Fig. 2), the air now starts to trail backward at different skew angle according to the speed of flight. Skew angle will increase due to increases in the forward flight speed and the rotating rotor starts to produces a roll-up trailing edge vortex both at advancing and retreating side. The blade-blade vortex interaction is clearly visible at high speed of flight and possible to greatly affect the blade at advancing side by increase the parasite drag.

Fig. 4 and Fig. 5 depicts the static pressure contour of rotor at element r/R = 0.75 and $\Psi = 180^o$ position. From these figures, the positive pressure is generated and acting at the lower surface while the negative pressure acting at the upper surface of the blade. The pressure increases when travel from root to the tip of the blade (Fig. 5). This is because at hovering mode, the blade element at inboard operates at lower airspeed than the blade element at the outboard portion. The generation of positive pressure at lower surface of the blade implies that there is a positive sign of vertical force or lift force generated by the blade for every flight speed.

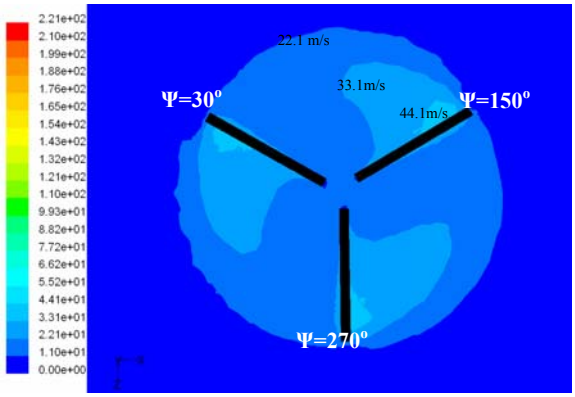

Fig. 1: Contour of Velocity Magnitude of 3 bladed Rotor at Hovering Mode (Plan View)

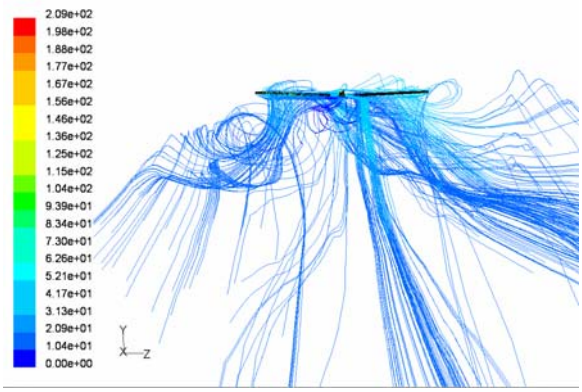

Fig. 2: Path Line of 4-bladed Rotor at Forward Flight Mode Coloured by Velocity Magnitude of V = 20 m/s (View at $\Psi = 0^o$)

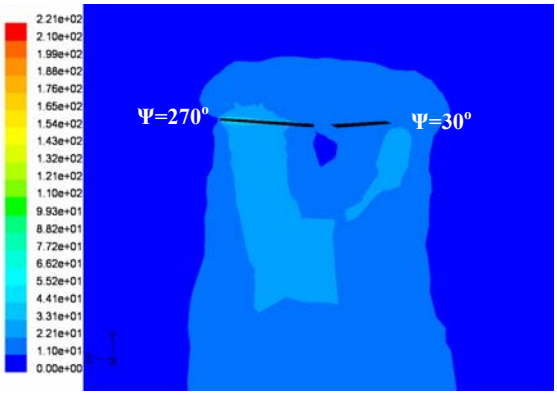

Fig. 3: Contour of Velocity Magnitude of 3 bladed Rotor at Hovering Mode (Side View).

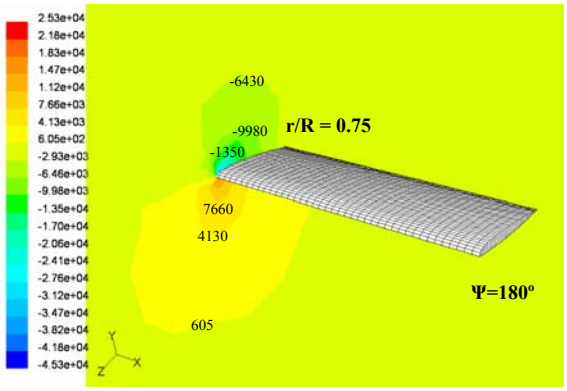

Fig. 4: Contour of Static Pressure of Hovering Rotor (measured at r/R= 0.75).

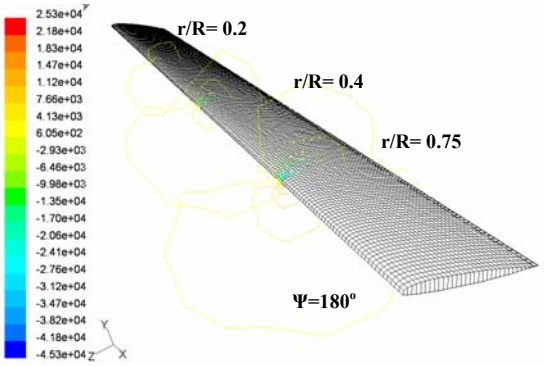

Figure 5: Contour of Static Pressure of Hovering Rotor (blade at Ψ = 180° position).

4.0 Conclusion

The isolated helicopter rotor of different rotor-engine combinations in hovering and forward flight was successful simulated using commercial computational fluid dynamic software FLUENT. Multiple references frame method was used on simulating the rotating rotor in hovering and forward flight modes. It was found from this study that the method applied in this simulation capable to provide good result on simulating a helicopter aerodynamic in these flight modes. The rise on the percentage of error (12-16%) on lift was observed for forward flight greater than 20 m/s. This error can be reduced by taking into account the dynamic motion of the rotating blades. This dynamic motion will be included in the future study on simulating a complete helicopter aerodynamic performance.

5.0 Acknowledgement

This study is supported by Malaysia Ministry of Science, Technology and Innovation (MOSTI) through the National Science Fellowship (NSF) scholarship programme.

6.0 References

[1] Caradonna, F. X. and Isom, M. P. (1972). "Subsonic and Transonic Potential Flow over Helicopter Rotor Blades", *AIAA Journal, No. 12, pp. 1606-1612.*

[2] Chang, I. C.(1984). "Transonic Flow Analysis for Rotors", *NASA TP 2375.*

[3] Xu, M., Mamou, M. and Khalid, M. (2002). "Numerical Investigation of Turbulent Flow Past a Four-Bladed Helicopter Rotor Using *k-ω* SST Model", *The 10th Annual Conference of CFD Society of Canada*, Windsor.

[4] Strawn, R. C. and Djomehri, M. J. (2001). "Computational Modeling of Hovering Rotor and Wake Aerodynamics," *American Helicopter Society 57th Annual Forum, Washington, DC.*

[5] Sides, J., Pahlke, K. and Costes, M. (2001). "Numerical Simulation of Flow Around Helicopter at DLR and ONERA", *Editions Scientifiques et Medicales Elsevier.*

[6] FLUENT News 2002 (11)2, pp: s9

[7] Prouty, R.W., 1986. *"Helicopter Performance, Stability, and Control"*, PWS Engineering, Boston.
[8] Leishman, G., 2002. *"Principles of Helicopter Aerodynamics"*. Cambridge Aerospace Series, United Kingdom.
[9] Wirogo, S., and Ruith, M., 2004. Virtual Blade Model-UGM 2004. 2004 CFD Summit.